Submission code: ZD6J8647DA

Elastic seismic modeling in vertically transversely isotropic media using decoupled elastic wave equations

Lucas Silva Bitencourt (CPGG - UFBA), Reynam Da Cruz Pestana (CPGG - UFBA)

Elastic seismic modeling in vertically transversely isotropic media using decoupled elastic wave equations

Please, do not insert author names in your submission PDF file.

Abstract Summary

To decrease the information loss when imaging a complex geological medium, it is crucial to consider anisotropy, particularly the transversely isotropic medium, as it is the most common anisotropy in exploration geophysics. However, the elastic wave equations that govern such medium describe P and S waves are coupled. This results in shear wave energy in seismic modeling and, consequently, in artifacts in the seismic image. Thus, the analytical decomposition of the elastic wave equation in the vertically transversely isotropic (VTI) media is proposed. The proposed equations correctly decouple the P and S wavefields. The efficacy of our method is demonstrated by modeling synthetic VTI data found in the literature.

Introduction

To enhance imaging, it is important to account for the anisotropy of the medium, as it influences both the kinematics and dynamics of the wavefield (Thomsen, 1986). Therefore, recent research efforts have focused on incorporating anisotropy, particularly vertically transversely isotropic (VTI) media, into seismic imaging (Bitencourt and Pestana, 2024; Pestana et al., 2012).

However, as conventional seismic imaging relies on acoustic or pseudo-acoustic equations, it does not account for the Earth's elastic nature. Moreover, these equations treat the elastic characteristics of the wavefield as noise (Feng and Schuster, 2017). Consequently, anisotropic elastic imaging has become a significant research focus in exploration geophysics. However, the coupling of P- and S-waves in elastic media introduces artifacts in the migrated image (Du et al., 2012).

Consequently, decoupling the P- and S-wavefields is crucial to improve the quality of seismic imaging without generating artifacts. For this purpose, different methods were proposed over the years. Recently, Zhang et al. (2022) proposed a notable anisotropic-Helmholtz decomposition method that numerically decouples the P and S wavefields and generates correct units, phases, and amplitudes compared with input elastic wavefields. Thus, in this work, we extend their work and propose the analytical decoupling of the 3D elastic wave equation in the VTI media.

Method

Let the 3D elastic VTI wave equation in the $\mathbf{k}-t$ domain in the matrix form,

$$\rho\frac{\partial^2\mathbf{U}}{\partial t^2} = -A\mathbf{U} + \mathbf{F}, \tag{1}$$

in which

$$c_{11} = (1+2\varepsilon)\,\rho v_P^2,\;\; c_{33} = \rho v_P^2,\;\; c_{44} = \rho v_S^2,\;\; c_{66} = (1+2\gamma)\,\rho v_S^2,$$
$$c_{13} = \rho\sqrt{\left[(1+2\delta)\,v_P^2 - v_S^2\right](v_P^2 - v_S^2)} - \rho v_S^2,$$
$$A = K_1^\dagger L_1 K_1 + K_2^\dagger L_2 K_2 + K_3^\dagger L_3 K_3 + K_4^\dagger L_3 K_4,$$
$$K_1 = \begin{bmatrix} ik_x & 0 & 0 \\ 0 & ik_y & 0 \\ 0 & 0 & ik_z \end{bmatrix}, K_2 = \begin{bmatrix} ik_y & 0 & 0 \\ 0 & ik_x & 0 \\ 0 & 0 & 0 \end{bmatrix}, K_3 = \begin{bmatrix} ik_z & 0 & 0 \\ 0 & 0 & 0 \\ 0 & 0 & ik_x \end{bmatrix}, K_4 = \begin{bmatrix} 0 & 0 & 0 \\ 0 & ik_z & 0 \\ 0 & 0 & ik_y \end{bmatrix}, \tag{2}$$
$$L_1 = \begin{bmatrix} c_{11} & (c_{11}-2c_{66}) & c_{13} \\ (c_{11}-2c_{66}) & c_{11} & c_{13} \\ c_{13} & c_{13} & c_{33} \end{bmatrix}, L_2 = \begin{bmatrix} c_{66} & c_{66} & c_{66} \\ c_{66} & c_{66} & c_{66} \\ c_{66} & c_{66} & c_{66} \end{bmatrix}, L_3 = \begin{bmatrix} c_{44} & c_{44} & c_{44} \\ c_{44} & c_{44} & c_{44} \\ c_{44} & c_{44} & c_{44} \end{bmatrix},$$

and ε, δ and γ are the Thomsen's parameters (Thomsen, 1986). Zhang et al. (2022) show that

$$\mathbf{U} = \mathbf{U}^P + \mathbf{U}^S,\;\; \mathbf{U}^P = DD^T\frac{1}{D^2}\mathbf{U},\;\; \mathbf{U}^S = \left(I - DD^T\frac{1}{D^2}\right)\mathbf{U}, \tag{3}$$

in which $\mathbf{U}^P$ and $\mathbf{U}^S$ are the P- and S-wave fields, and $D = \begin{bmatrix} k_x & k_y & rk_z \end{bmatrix}^T$, in which $r = \frac{\sqrt{\left[(1+2\delta)v_P^2 - v_S^2\right](v_P^2 - v_S^2)}}{(1+2\varepsilon)v_P^2 - v_S^2}$. Hence, we apply equation 3 to equation 1 and obtain

$$\rho\frac{\partial^2\mathbf{U}^P}{\partial t^2} = -DD^T\frac{1}{D^2}\left[A\mathbf{U} - \mathbf{F}\right],\;\; \rho\frac{\partial^2\mathbf{U}^S}{\partial t^2} = -\left(I - DD^T\frac{1}{D^2}\right)\left[A\mathbf{U} - \mathbf{F}\right]. \tag{4}$$

Thus, by substituting equations 2 into equation 4 and taking the inverse Fourier transform, we obtain the decoupled 3D elastic VTI pure P-wave equation in the $\mathbf{x} - t$ domain

$$\begin{aligned}
w_x =& -\mathfrak{F}^{-1}\Bigg\{\frac{1}{k_x^2 + k_y^2 + r^2k_z^2}\mathfrak{F}\Bigg\{\frac{\partial}{\partial x}\left[c_{11}\frac{\partial}{\partial x}\mathbf{u}_x + (c_{11}-2c_{66})\frac{\partial}{\partial y}\mathbf{u}_y + c_{13}\frac{\partial}{\partial z}\mathbf{u}_z\right] \\
&+ \frac{\partial}{\partial y}\left[c_{66}\left(\frac{\partial}{\partial y}\mathbf{u}_x + \frac{\partial}{\partial x}\mathbf{u}_y\right)\right] + \frac{\partial}{\partial z}\left[c_{44}\left(\frac{\partial}{\partial z}\mathbf{u}_x + \frac{\partial}{\partial x}\mathbf{u}_z\right)\right]\Bigg\}\Bigg\}, \\
w_y =& -\mathfrak{F}^{-1}\Bigg\{\frac{1}{k_x^2 + k_y^2 + r^2k_z^2}\mathfrak{F}\Bigg\{\frac{\partial}{\partial y}\left[(c_{11}-2c_{66})\frac{\partial}{\partial x}\mathbf{u}_x + c_{11}\frac{\partial}{\partial y}\mathbf{u}_y + c_{13}\frac{\partial}{\partial z}\mathbf{u}_z\right] \\
&+ \frac{\partial}{\partial x}\left[c_{66}\left(\frac{\partial}{\partial y}\mathbf{u}_x + \frac{\partial}{\partial x}\mathbf{u}_y\right)\right] + \frac{\partial}{\partial z}\left[c_{44}\left(\frac{\partial}{\partial z}\mathbf{u}_y + \frac{\partial}{\partial y}\mathbf{u}_z\right)\right]\Bigg\}\Bigg\}, \\
w_z =& -\mathfrak{F}^{-1}\Bigg\{\frac{1}{k_x^2 + k_y^2 + r^2k_z^2}\mathfrak{F}\Bigg\{\frac{\partial}{\partial z}\left[c_{13}\frac{\partial}{\partial x}\mathbf{u}_x + c_{13}\frac{\partial}{\partial y}\mathbf{u}_y + c_{33}\frac{\partial}{\partial z}\mathbf{u}_z\right] \\
&+ \frac{\partial}{\partial x}\left[c_{44}\left(\frac{\partial}{\partial z}\mathbf{u}_x + \frac{\partial}{\partial x}\mathbf{u}_z\right)\right] + \frac{\partial}{\partial y}\left[c_{44}\left(\frac{\partial}{\partial z}\mathbf{u}_y + \frac{\partial}{\partial y}\mathbf{u}_z\right)\right]\Bigg\}\Bigg\}, \\
\rho\frac{\partial^2\mathbf{u}^P}{\partial t^2} =& \begin{bmatrix} \frac{\partial}{\partial x} & \frac{\partial}{\partial y} & r\frac{\partial}{\partial z} \end{bmatrix}^T\left(\frac{\partial w_x}{\partial x} + \frac{\partial w_y}{\partial y} + r\frac{\partial w_z}{\partial z}\right),
\end{aligned} \tag{5}$$

in which $\mathfrak{F}$ and $\mathfrak{F}^{-1}$ are the direct and inverse Fourier transforms respectively, and the decoupled 3D elastic VTI pure S-wave equation in the $\mathbf{x} - t$ domain

$$\rho\frac{\partial^2\mathbf{u}^S}{\partial t^2} = \rho\frac{\partial^2\mathbf{u}}{\partial t^2} - \rho\frac{\partial^2\mathbf{u}^P}{\partial t^2}. \tag{6}$$

Note that, although the P- and S-wave fields are decoupled, their equations are coupled, as $\mathbf{u} = \mathbf{u}^P + \mathbf{u}^S$. Moreover, note that the decoupling operators are also applied to the source functions. Finally, to compute $\frac{1}{k_x^2+k_y^2+r^2k_z^2}$, we follow the approach of Zhang et al. (2022).

Results

To verify the proposed methods, the anisotropic elastic modeling of the 2D Hess VTI-elastic model is implemented. The wavefield is propagated for $t = 0.65\,\mathrm{s}$, with $\Delta t = 1\,\mathrm{ms}$ and a peak frequency of $12.5\,\mathrm{Hz}$. For comparison, equation 1 and the decoupling method proposed by Zhang et al. (2022) are also used for modeling.

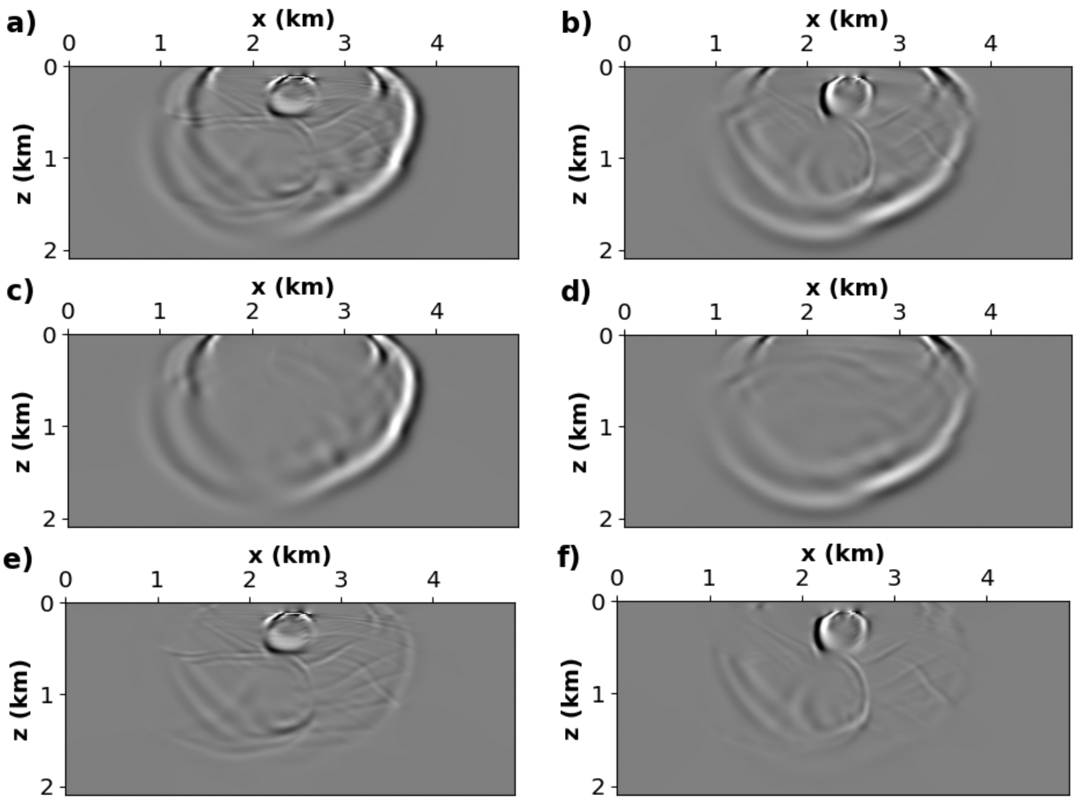

Figure 1: Comparison of wavefield snapshots at time $t = 0.65\,\mathrm{s}$: a) X and b) Z components computed with equation 1; c) X and d) Z components of the pure P-wavefield; and e) X and f) Z components of the pure S-wavefield.

Figure 1 shows a comparison of snapshots computed with equation 1 and with the proposed equations; and Figure 2 shows a profile extracted at $x = 1800\,\mathrm{m}$, in which the result obtained using decoupling method from Zhang et al. (2022) is added. It can be seen that the proposed equations provide a stable and consistent result. Furthermore, they provide a better amplitude matching close to the border in relation to the method developed by Zhang et al. (2022), as seen in the profiles.

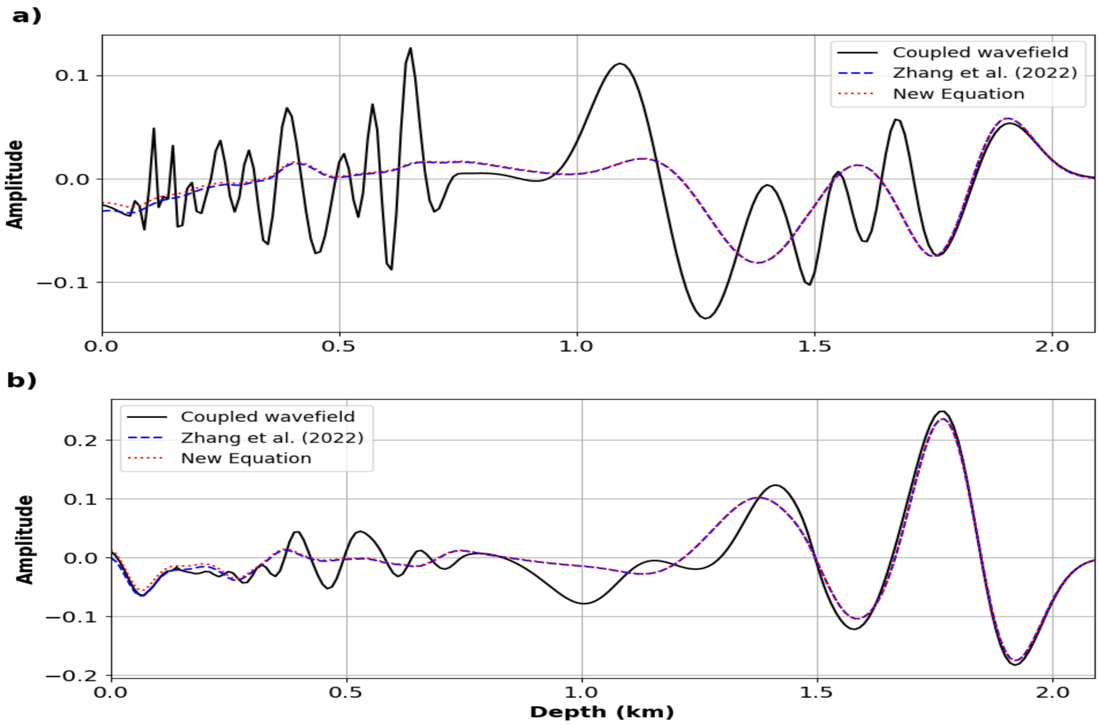

Figure 2: Profile extracted from wavefield at $x = 1800\,\mathrm{m}$ and $t = 0.65\,\mathrm{s}$: a) X and b) Z components.

Conclusions

In this study, the analytical decomposition of the 3D elastic wave equation in VTI media was presented. Therewith, the 3D pure P-wave equation in VTI media was proposed. It is shown that the new equations correctly decouple the P and S wavefields. Additionally, we have shown that they are efficacious and stable for seismic modeling of complex inhomogeneous and anisotropic media. These results are significant, as they can improve the quality of seismic imaging.

References

Bitencourt, L. S., and R. C. Pestana, 2024, Simplified TTI pure qP-wave equation implemented in the space domain and applied for reverse time migration in TTI media: Geophysics, **89**, no. 1, C17–C28.

Du, Q., Y. Zhu, , and J. Ba, 2012, Polarity reversal correction for elastic reverse time migration: Geophysics, **77**, S31—-S41.

Feng, Z., and G. T. Schuster, 2017, Elastic least-squares reverse time migration: Geophysics, **82**, S143—-S157.

Pestana, R. C., B. Ursin, and P. L. Stoffa, 2012, Rapid expansion and pseudo spectral implementation for reverse time migration in VTI media: Journal of Geophysics and Engineering, **9**, no. 3, 291–301.

Thomsen, L., 1986, Weak elastic anisotropy: Geophysics, **51**, 1954–1966.

Zhang, L., L. Liu, F. Niu, J. Zuo, D. Shuai, W. Jia, and Y. Zhao, 2022, A novel and efficient engine for P-/S-wave-mode vector decomposition for vertical transverse isotropic elastic reverse time migration: Geophysics, **87**, no. 4, S185–S207.